2. K. B. Beckman and B. N. Ames, *Physiol. Rev.* **78**, 547 (1998).
3. W. C. Orr and R. S. Sohal, *Science* **263**, 1128 (1994); T. L. Parkes *et al.*, *Nature Genet.* **19**, 171 (1998).
4. S. Ogg *et al.*, *Nature* **389**, 994 (1997); K. Lin, J. B. Dorman, A. Rodan, C. Kenyon, *Science* **278**, 1319 (1997); S. Paradis and G. Ruvkun, *Genes Dev.* **12**, 2488 (1998); H. A. Tissenbaum and G. Ruvkun, *Genetics* **148**, 703 (1998).
5. T. E. Johnson, *Science* **249**, 908 (1990); S. Murakami and T. E. Johnson, *Genetics* **143**, 1207 (1996); Y.-J. Lin, L. Seroude, S. Benzer, *Science* **282**, 943 (1998).
6. C. E. Yu *et al.*, *Science* **272**, 258 (1996); L. Ye *et al.*, *Am. J. Med. Genet.* **68**, 494 (1997).
7. R. Weindruch and R. L. Walford, *The Retardation of Aging and Disease by Dietary Restriction* (Thomas, Springfield, IL, 1988).
8. C. Dutta, E. C. Hadley, J. Lexell, *Muscle Nerve* **5**, S5 (1997).
9. R. Ludatscher, M. Silberman, D. Gershon, A. Reznick, *Exp. Gerontol.* **18**, 113 (1983).
10. Methods used to house and feed male C57BL/6 mice, a commonly used model in aging research with an average life-span of ~30 months, were recently described [T. D. Pugh, T. D. Oberley, R. Weindruch, *Cancer Res.* **59**, 642 (1999)].
11. Total RNA was extracted from frozen tissue by using TRIZOL reagent (Life Technologies). Polyadenylate [poly(A)$^+$] RNA was purified from the total RNA with oligo-dT–linked Oligotex resin (Qiagen). One microgram of poly(A)$^+$ RNA was converted into double-stranded cDNA (ds-cDNA) by using SuperScript Choice System (Life Technologies) with an oligo-dT primer containing a T7 RNA polymerase promoter (Genset). After second-strand synthesis, the reaction mixture was extracted with phenol–chloroform–isoamyl alcohol, and ds-cDNA was recovered by ethanol precipitation. In vitro transcription was performed by using a T7 Megascript Kit (Ambion) with 1.5 μl of ds-cDNA template in the presence of a mixture of unlabeled ATP, CTP, GTP, and UTP and biotin-labeled CTP and UTP [bio-11-CTP and bio-16-UTP (Enzo)]. Biotin-labeled cRNA was purified by using an RNeasy affinity column (Qiagen), and fragmented randomly to sizes ranging from 35 to 200 bases by incubating at 94°C for 35 min. The hybridization solutions contained 100 mM MES, 1 M Na$^+$, 20 mM EDTA, and 0.01% Tween 20. The final concentration of fragmented cRNA was 0.05 μg/μl in the hybridization solutions. After hybridization, the hybridization solutions were removed and the gene chips were washed and stained with streptavidin-phycoerythrin. DNA chips were read at a resolution of 6 μm with a Hewlett-Packard GeneArray Scanner.
12. Detailed protocols for data analysis of Affymetrix microarrays and extensive documentation of the sensitivity and quantitative aspects of the method have been described [D. J. Lockhart, *Nature Biotechnol.* **14**, 1675 (1996)]. Briefly, each gene is represented by the use of ~20 perfectly matched (PM) and mismatched (MM) control probes. The MM probes act as specificity controls that allow the direct subtraction of both background and cross-hybridization signals. The number of instances in which the PM hybridization signal is larger than the MM signal is computed along with the average of the logarithm of the PM:MM ratio (after background subtraction) for each probe set. These values are used to make a matrix-based decision concerning the presence or absence of an RNA molecule. Positive average signal intensities after background subtraction were observed for over 4000 genes for all samples. To determine the quantitative RNA abundance, the average of the differences representing PM minus MM for each gene-specific probe family is calculated, after discarding the maximum, the minimum, and any outliers beyond 3 SDs. Averages of pairwise comparisons were made between animals with Affymetrix software. To determine the effect of age, each 5-month-old mouse ($n = 3$) was compared to each 30-month-old ($n = 3$) mouse, generating a total of nine pairwise comparisons. To determine the effect of diet, 30-month-old CR-fed ($n = 3$) and 30-month-old control-fed ($n = 3$) animals were similarly compared. Pearson correlation coeficients were calculated between individual animals in the same age/diet groups. No correlation coeficient between two animals in the same age/diet group was less than 0.98.
13. M. H. Goyns *et al.*, *Mech. Ageing Dev.* **101**, 73 (1998).
14. J. Jackman, I. Alamo Jr., A. J. Fornace Jr., *Cancer Res.* **54**, 5656 (1994).
15. O. Stachowiak, M. Dolder, T. Wallimann, C. Richter, *J. Biol. Chem.* **273**, 16694 (1998).
16. L. Larsson, *J. Gerontol. Biol. Sci.* **50A**, 96 (1995); J. Lexell, *J. Nutr.* **127**, 1011S (1997).
17. J. C. Copray and N. Brouwer, *Neurosci. Lett.* **236**, 41 (1997).
18. G. Marazzi and K. M. Buckley, *Dev. Dyn.* **197**, 115 (1993).
19. C. A. Peterson and J. D. Houle, *J. Nutr.* **127**, 1007S (1997).
20. M. Shibanuma, J. Mashimo, T. Kuroki, K. Nose, *J. Biol. Chem.* **269**, 26767 (1994); S. Wang, E. J. Moerman, R. A. Jones, R. Thweatt, S. Goldstein, *Mech. Ageing Dev.* **92**, 121 (1996).
21. ATP synthase: W. Junge, H. Lill, S. Engelbrecht, *Trends Biochem. Sci.* **22**, 420 (1997); NADP transhydrogenase: J. B. Hoek and J. Rydstrom, *Biochem. J.* **254**, 1 (1988); LON protease: K. Luciakova, B. Sokolikova, M. Chloupkova, B. D. Nelson, *FEBS Lett.* **444**, 186 (1999); ERV1: T. Lisowsky, *Curr. Genet.* **26**, 15 (1994).
22. A. L. Schwartz and A. Ciechanover, *Annu. Rev. Med.* **50**, 57 (1999).
23. J. L. DeRisi, V. R. Iyer, P. O. Brown, *Science* **278**, 680 (1997).
24. J. R. Zierath *et al.*, *Endocrinology* **139**, 5034 (1998).
25. T. Tomoyasu, T. Ogura, T. Tatsuta, B. Bukau, *Mol. Microbiol.* **30**, 567 (1998); T. Yura, H. Nagai, H. Mori, *Annu. Rev. Microbiol.* **47**, 321 (1993).
26. L. Wikstrom *et al.*, *EMBO J.* **17**, 455 (1998).
27. E. R. Stadtman, *Science* **257**, 1220 (1992).
28. R. S. Sohal and R. Weindruch, *ibid.* **273**, 59 (1996).
29. Supported by NIH grants PO1 AG11915 (R.W.) and RO1 CA78723 (T.A.P.). T.A.P. is a recipient of the Shaw Scientist (Milwaukee Foundation) and Burroughs Wellcome Young Investigator awards.

Dual Function of the Selenoprotein PHGPx During Sperm Maturation

Fulvio Ursini,[1] **Sabina Heim,**[2] **Michael Kiess,**[2] **Matilde Maiorino,**[1] **Antonella Roveri,**[1] **Josef Wissing,**[2] **Leopold Flohé**[3]*

The selenoprotein phospholipid hydroperoxide glutathione peroxidase (PHGPx) changes its physical characteristics and biological functions during sperm maturation. PHGPx exists as a soluble peroxidase in spermatids but persists in mature spermatozoa as an enzymatically inactive, oxidatively cross-linked, insoluble protein. In the midpiece of mature spermatozoa, PHGPx protein represents at least 50 percent of the capsule material that embeds the helix of mitochondria. The role of PHGPx as a structural protein may explain the mechanical instability of the mitochondrial midpiece that is observed in selenium deficiency.

Selenium is essential for male fertility in rodents and has also been implicated in the fertilization capacity of spermatozoa of livestock and humans (*1*). Selenium deficiency is associated with impaired sperm motility, structural alterations of the midpiece, and loss of flagellum (*1*). However, three decades after the discovery of selenium as an integral constituent of redox enzymes (*2*), the molecular basis of the relationship of the essential trace element and male fertility remains obscure. The selenoprotein PHGPx (Enzyme Commission number 1.11.1.12) is abundantly expressed in spermatids and displays high activity in postpubertal testis (*3*). In mature spermatozoa, however, selenium is largely restricted to the mitochondrial capsule, a keratin-like matrix that embeds the helix of mitochondria in the sperm midpiece (*4*). A "sperm mitochondria–associated cysteine-rich protein (SMCP)" (*5*) had been considered to be the selenoprotein accounting for the selenium content of the mitochondrial capsule (*4–6*). The rat SMCP gene, however, does not contain an in-frame TGA codon (*7*) that would enable a selenocysteine incorporation (*8*). In mice, the three in-frame TGA codons of the SMCP gene are upstream of the translation start (*5*). SMCP can therefore no longer be considered as a selenoprotein. Instead, the "mitochondrial capsule selenoprotein (MCS)," as SMCP was originally referred to (*4–7*), is here identified as PHGPx.

Routine preparations of rat sperm mitochondrial capsules (*9*) yielded a fraction that was insoluble in 1% SDS containing 0.2 mM dithiothreitol (DTT) and displayed a vesicular appearance in electron microscopy (Fig. 1A). The vesicles readily disintegrated upon exposure to 0.1 M mercaptoethanol (Fig. 1B) and became fully soluble in 6 M guanidine-HCl. When the solubilized capsule material was subjected to polyacrylamide gel electrophoresis (PAGE), four bands in the 20-kD

[1]Dipartimento di Chimica Biologica, Università di Padova, Viale G. Colombo 3, I-35121 Padova, Italy. [2]National Research Centre for Biotechnology (GBF), Mascheroder Weg 1, D-38124 Braunschweig, Germany. [3]Department of Biochemistry, Technical University of Braunschweig, Mascheroder Weg 1, D-38124 Braunschweig, Germany.

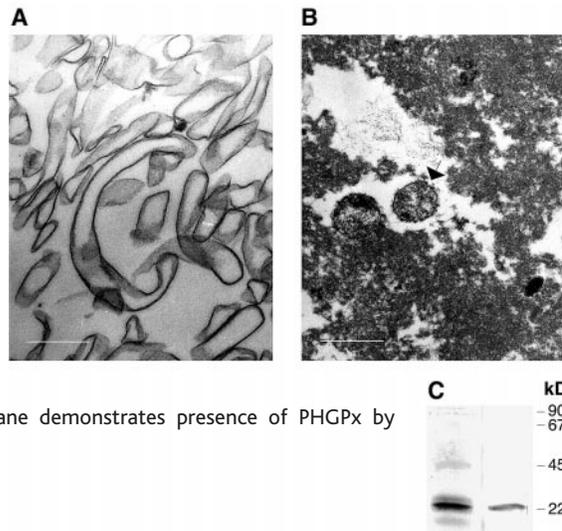*To whom correspondence should be addressed. E-mail: lfl@gbf.de

region were detected (Fig. 1C, left lane). Protein immunoblotting (*10*) revealed that the most prominent band reacted with PHGPx antibodies (Fig. 1C, right lane). NH_2-terminal sequencing (*11*) of the 21-kD band (46% of total protein content according to stain intensity) revealed that it consisted of at least 95% p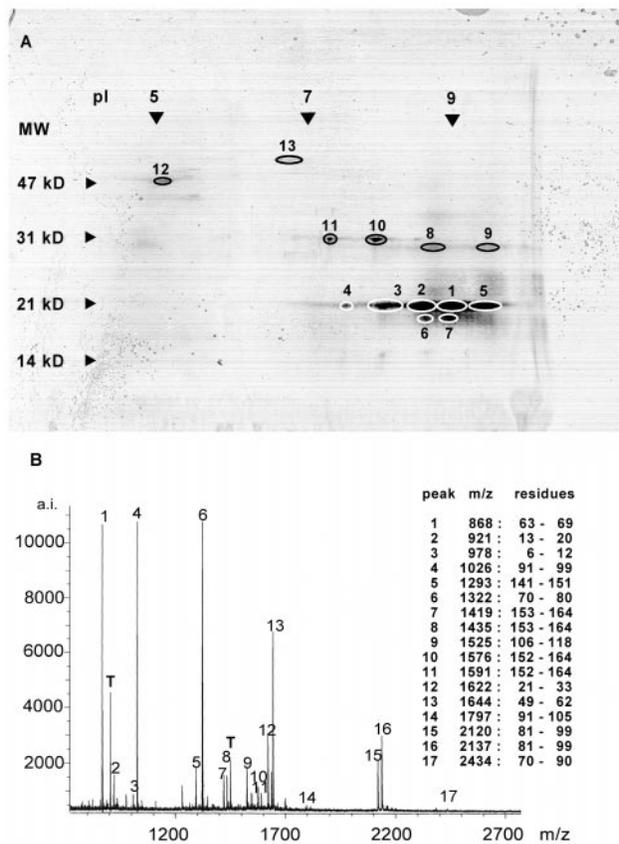ure PHGPx. We therefore investigated the composition of the mitochondrial capsules by two-dimensional (2D) electrophoresis (*12*) (Fig. 2A) followed by microsequencing (*13*) or matrix-assisted laser desorption ionization time-of-flight (MALDI-TOF) analysis (*14*) for identification (Fig. 2B). The spot migrating with an apparent molecular mass of 21 kD and focusing at a pH near 8 (spot 3) proved to be PHGPx, according to the masses of tryptic peptides detected by MALDI-TOF spectrometry (Fig. 2B). All tryptic fragments yielding MALDI-TOF signals of high intensity could be attributed to PHGPx or trypsin. The predicted NH_2-terminal (positions 3 to 12) and COOH-terminal peptides (positions 165 to 170), the fragment corresponding to positions 100 to 105, and those expected from the basic sequence part (residues 119 to 151) were too small to be reliably identified. The fragment corresponding to positions 34 to 48 comprising the active site selenocysteine was not detected either. The more acidic spot 4 of Fig. 2A, the more basic spots 1, 2, and 5, and those exhibiting a smaller apparent molecular mass (spots 6 and 7) also contained PHGPx (*15*). Spots 1 to 6 were essentially homogeneous. Spot 7 showed a trace of impurity that could not be identified by masses of fragments. Integrated stain intensities of the individual spots indicate that PHGPx constituted about 50% of the capsule material.

Minor components present in the gel (Fig. 2A, spots 10 to 13) were assigned to mitochondrial proteins or to cytosolic contaminations. Spots 8 and 9 consisted of "outer dense fiber protein," a cysteine-rich structural sperm protein that is associated with the helix of mitochondria in the midpiece but also extends into the flagellum. SMCP was not detected. This basic protein that becomes superficially associated with the outer mitochondrial membranes in late spermatids and epididymal spermatozoa (*5*) might have been degraded by trypsination during capsule preparation.

PHGPx was enzymatically inactive in mature spermatozoa prepared from the tail of the epididymis and was not reactivated by the reduced form of glutathione (GSH) in the low

Fig. 1. Presence of PHGPx in the mitochondrial capsule of rat spermatozoa. (**A**) Mitochondrial capsule prepared by trypsination and centrifugation (*4, 9*). (**B**) The same preparation as shown in (A) but after exposure to 0.1 M 2-mercaptoethanol for 15 min at 4°C. Contamination of the capsule material by mitochondria is evident from the presence of mitochondrial ghosts (arrowhead). Scale bars, 0.3 μm. (**C**) SDS-PAGE of proteins extracted from capsule material by treatment with 0.1 M 2-mercaptoethanol, 0.1 M tris-HCl (pH 7.5), and 6 M guanidine-HCl. Left lane is stained with colloidal gold; right lane demonstrates presence of PHGPx by protein immunoblotting (*10*).
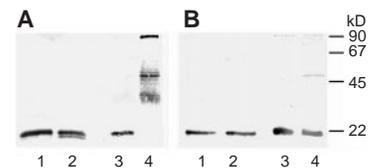

Fig. 2. Analysis of the composition of the mitochondrial capsule of spermatozoa. (**A**) Two-dimensional electrophoresis of purified dissolved capsule material. Proteins were focused in a linear pH gradient from 3 to 10 (horizontal direction), then reduced, amidocarboxymethylated, subjected to SDS electrophoresis, and stained with Coomassie blue. MALDI-TOF analysis of the visible spots identified the following proteins (NCBI database): spots 1 to 7, PHGPx (accession number 544434); spots 8 and 9, outer dense fiber protein (accession number P21769); spots 10 and 11, voltage-dependent anion channel-like protein (accession number 540011); spot 12, "stress-activated protein kinase" (accession number 493207); spot 13, glycerol-3-phosphate dehydrogenase (accession number P35571) (*22*). (**B**) MALDI-TOF spectrum (overview) of tryptic peptides obtained from PHGPx as found in spot 3. Abscissa, mass/charge ratio (*m/z*) of the peptide fragments; ordinate, arbitrary units of intensity (a.i.). The insert lists the mass signals 1 to 17 attributed to tryptic fragments of PHGPx with measured *m/z* values and corresponding residues in the PHGPx sequence. Peaks 8 and 11 correspond to tryptic fragments with oxidized methionine residue; peak 15 corresponds to a fragment with an NH_2-terminal pyroglutamyl residue. T, trypsin-derived fragments.

peak	m/z	residues
1	868 :	63 - 69
2	921 :	13 - 20
3	978 :	6 - 12
4	1026 :	91 - 99
5	1293 :	141 - 151
6	1322 :	70 - 80
7	1419 :	153 - 164
8	1435 :	153 - 164
9	1525 :	106 - 118
10	1576 :	152 - 164
11	1591 :	152 - 164
12	1622 :	21 - 33
13	1644 :	49 - 62
14	1797 :	91 - 105
15	2120 :	81 - 99
16	2137 :	81 - 99
17	2434 :	70 - 90

Fig. 3. Formation of PHGPx-containing aggregates by H_2O_2 in the absence of GSH. (**A**) Whole rat spermatozoa were solubilized with 0.1 M 2-mercaptoethanol and 6 M guanidine-HCl and freed from low molecular weight compounds as described (*17*). Aliquots of the protein mixture (0.05 mg of protein) were subjected to SDS-PAGE under reducing (lanes 1 and 2) and nonreducing conditions (lanes 3 and 4) at zero time (lanes 1 and 3) or after 15-min exposure to 75 μM H_2O_2 (lanes 2 and 4). PHGPx-containing bands were detected by protein immunoblotting (*10*). (**B**) Lanes 1 to 4 show the same experiments but performed with purified rat testis PHGPx adjusted to the PHGPx content in solubilized spermatozoal proteins. Only traces of dimerized PHGPx and aggregates are seen in the sample exposed to H_2O_2 for 15 min (lane 4).

millimolar range, as used under conventional test conditions (*16*). High concentrations of thiols (0.1 M 2-mercaptoethanol or DTT), which in the presence of guanidine fully dissolved the capsule, regenerated a substantial PHGPx activity (*17*). In fact, the specific activities thereby obtained from mitochondrial capsules (5600 ± 290 mU/mg protein) exceeded, by a factor of 20, the values measured in spermatogenic cells (250 ± 10 mU/mg). Nevertheless, the PHGPx activity regenerated from the capsule material was low relative to its PHGPx protein content. On the basis of the specific activity of pure PHGPx, the reactivated enzyme would be equivalent to less than 3% of the capsule protein, whereas the 2D electrophoresis suggested a PHGPx protein content of at least 50%. The increase of PHGPx activity by the reductive procedure was similarly observed in epididymal spermatozoa (from zero to 3140 ± 200 mU/mg protein) but not in spermatogenic cells from testicular tubules (250 ± 10 to 260 ± 10 mU/mg). The latter observation is consistent with the expression of PHGPx as active peroxidase in round spermatids (*3*). The switch of PHGPx from a soluble active enzyme to an enzymatically inactive structural protein thus occurs during differentiation of spermatids into spermatozoa (*18*).

The alternate roles of PHGPx as a glutathione-dependent hydroperoxide reductase or a structural protein are not necessarily unrelated. A feature common to all glutathione peroxidases is a selenocysteine residue, which, together with a tryptophan and a glutamine residue, forms a catalytic triad (*19*). Therein the selenol group of the selenocysteine residue is oxidized by hydroperoxides with high rate constants. The reaction product, a selenenic acid derivative, R-SeOH, reacts with GSH to form a selenadisulfide bridge between enzyme and substrate, R-Se-S-G, from which the ground-state enzyme is regenerated by a second GSH. In analogy, PHGPx, which is the least specific of the glutathione peroxidases (*19*), can use protein thiols as alternate substrates to create protein aggregates that are cross-linked by selenadisulfide or disulfide bonds. This likely occurs when cells are exposed to hydroperoxides at low concentrations of GSH, as is documented for late stages of spermatogenesis (*20*). Proteins derived from epididymal spermatozoa, when exposed to H_2O_2 in the absence of GSH, yielded a variety of PHGPx-containing aggregates (Fig. 3A). This process depends on the presence of thiol groups in proteins distinct from PHGPx, because under identical conditions only a marginal aggregate formation was observed with pure PHGPx (Fig. 3B).

Our findings require a fundamental reconsideration of the role of selenium in male fertility. The predominance of the selenoprotein PHGPx in the male reproductive system (*3*) has been believed to reflect the necessity to shield germ line cells from oxidative damage by hydroperoxides (*3, 20*). This concept still merits attention with regard to the mutagenic potential of hydroperoxides and probably holds true for the early phases of spermatogenesis. At this stage, phenomena attributed to the enzymatic activity of PHGPx or other glutathione peroxidases—for instance, silencing lipoxygenases, dampening the activation of nuclear factor κB, or inhibiting apoptosis (*21*)—may also be relevant. Mature spermatozoa, however, depend on PHGPx as a structural protein, because the morphological midpiece alterations that are observed in selenium deficiency likely result from impaired biosynthesis of the selenoprotein. In consequence, it is not the antioxidant capacity of PHGPx but the ability to use hydroperoxides for the formation of a structural element of the spermatozoon that is pivotal for male fertility.

References and Notes

1. D. G. Brown and R. F. Burk, *J. Nutr.* **103**, 102 (1973); A. S. H. Wu, J. E. Oldfield, L. R. Shull, P. R. Cheeke, *Biol. Reprod.* **20**, 793 (1979); E. Wallace, H. I. Calvin, K. Ploetz, G. W. Cooper, in *Selenium in Biology and Medicine*, G. F. Combs, O. A. Levander, J. E. Spallholz, J. E. Oldfield, Eds. (AVI, Westport, CT, 1987), pp. 181–196; D. Behne, H. Weiler, A. Kyriakopoulos, *J. Reprod. Fertil.* **106**, 291 (1996); National Research Council Subcommittee on Selenium, *Selenium in Nutrition* (National Academy Press, Washington, DC, 1983).
2. J. T. Rotruck *et al.*, *Science* **179**, 588 (1973); L. Flohé, W. A. Günzler, H. H. Schock, *FEBS Lett.* **32**, 132 (1973); D. C. Turner and T. C. Stadtman, *Arch. Biochem. Biophys.* **154**, 366 (1973); J. R. Andreesen and L. G. Ljungdahl, *J. Bacteriol.* **116**, 867 (1973).
3. A. Roveri *et al.*, *J. Biol. Chem.* **267**, 6142 (1992); A. Giannattasio, M. Girotti, K. Williams, L. Hall, A. J. Bellastella, *J. Endocrinol. Invest.* **20**, 439 (1997); M. Maiorino *et al.*, *FASEB J.* **12**, 1359 (1998).
4. H. I. Calvin, G. W. Cooper, E. Wallace, *Gamete Res.* **4**, 139 (1981).
5. L. Cataldo, K. Baig, R. Oko, M. A. Mastrangelo, K. C. Kleene, *Mol. Reprod. Dev.* **45**, 320 (1996).
6. V. Pallini and E. Bacci, *J. Submicr. Cytol.* **11**, 165 (1979); S.-Y. Nam, H.-Y. Youn, K. Ogawa, M. Kurohmaru, Y. Hayashi, *J. Reprod. Dev.* **43**, 227 (1997).
7. I. M. Adham *et al.*, *DNA Cell Biol.* **15**, 159 (1996).
8. T. C. Stadtman, *Annu. Rev. Biochem.* **59**, 111 (1990); J. Heider, Ch. Baron, A. Böck, *EMBO J.* **11**, 3759 (1992); M. J. Berry, L. Banu, J. W. Harney, P. R. Larsen, *ibid.* **12**, 3315 (1993); L. Flohé, E. Wingender, R. Brigelius-Flohé, in *Oxidative Stress and Signal Transduction*, H. J. Forman and E. Cadenas, Eds. (Chapman & Hall, New York, 1997), pp. 415–440.
9. Spermatozoa of 4-month-old Wistar rats were collected by squeezing the cauda epididymis and vas deferens in phosphate-buffered saline (PBS) and centrifuged at 600*g* for 10 min. Spermatogenic cells were prepared as described [M. L. Meistrich, J. Longtin, W. A. Brock, S. R. Grimes, M. L. Mace, *Biol. Reprod.* **25**, 1065 (1981)]. Sperm mitochondrial capsule was prepared according to (*4*).
10. Proteins were blotted onto nitrocellulose, probed with an antigen-purified rabbit antibody raised against pig heart PHGPx, and detected by biotinylated antibody to rabbit immunoglobulin G (IgG) and streptavidin alkaline phosphatase complex.
11. Before NH_2-terminal sequencing, proteins were blotted onto polyvinylidene difluoride membranes for 16 hours at pH 8.3 (25 mM tris-HCl, 192 mM glycine) and 100 mA (30 V).
12. Mitochondrial capsule material (100 μg) was dissolved in 400 μl of a solution containing 7 M urea, 2 M thiourea, 4% CHAPS, 40 mM DTT, 20 mM tris base, and 0.5% IPG buffer (Pharmacia) and focused in an IPG-phor (Pharmacia) at 20°C by stepwise increasing voltage up to 5000 V at <30 μA per IPG strip. The pH gradient was nonlinear from 3 to 10 or linear from 3 to 10 or 6 to 11. The focused IPG strips were equilibrated for SDS-PAGE with a solution containing 60 mM DTT in 6 M urea, 30% glycerol, and 0.05 M tris-HCl buffer (pH 8.8), and thereafter with the same buffer containing 250 mM iodoacetamide instead of DTT. Gels were stained with Coomassie blue.
13. Protein spots from 1.5-mm 2D gels were digested with modified trypsin (Promega, sequencing grade) in 25 mM $(NH_4)HCO_3$ overnight at 37°C. The digests were extracted twice, dried, and reconstituted in 10 μl of water. Peptides were separated on a reversed-phase capillary column (0.5 mm × 150 mm) with a gradient of acetonitrile in 0.1% formic acid/4 mM ammonium acetate at a flow rate of 5 μl/min. Aliquots of 5 μl were spotted onto Biobrene-treated glass fiber filters and sequenced on an Applied Biosystems 494A sequencer with standard pulsed liquid cycles.
14. Spots were cut out from gels, neutralized with $(NH_4)HCO_3$, destained with 400 μl of 50% acetonitrile/10 mM $(NH_4)HCO_3$, and dried in a Speed Vac Concentrator (Savant). Protein was digested overnight by sequencing grade trypsin (2 ng/μl, Promega) in 50 mM $(NH_4)HCO_3$. Digests were extracted with 60% acetonitrile/40% H_2O/0.1% trifluoroacetic acid, lyophilized, desalted on RP18 columns, eluted with saturated α-hydroxy-4-cyano-cinnamic acid, and loaded onto the MALDI target [J. Gobom, E. Nordhoff, R. Ekman, P. Roepstorff, *Int. J. Mass Spectrom.* **169–170**, 153 (1998)]. Reflectron MALDI mass spectra were recorded on a Reflex MALDI-TOF mass spectrometer (Bruker-Franzen-Analytik, Bremen). Ions were accelerated at 20 kV and reflected at 21.3 kV. Spectra were externally calibrated using the monoisotopic MH^+ ion from two peptide standards; 100 to 200 laser shots were summed for each spectrum. Mass identification was performed with MS-Fit (http://falcon.ludwig.ucl.ac.uk/ucsfhtml3.2/msfit.htm).
15. Masses of tryptic fragments covering the positions of the PHGPx sequence 21 to 33, 49 to 99, 106 to 118, and 141 to 151 were identified by MALDI-TOF analysis in spots 1 to 7 (Fig. 2A). Sequence coverage was about 75%. Recovery of fragments comprising residues 3 to 9 and 165 to 170 (COOH-terminus) varied between spots. Five distinct spots in the 20-kD region were also separated using a thicker 2D gel developed with a nonlinear gradient from pH 3 to 10. Here, the presence of PHGPx was verified by sequencing major tryptic peptides. Again, the five spots representing PHGPx were the most abundant ones in the gel. The chemical modifications of PHGPx leading to distinct differences in charge and size were not elucidated. Sequencing revealed an identical NH_2-terminus of the size isomers starting with Ala-Ser-Arg-Asp-Asp-Trp-Arg-Cys-Ala-Arg, a sequence either corresponding to the originally proposed translation start [R. Brigelius-Flohé *et al.*, *J. Biol. Chem.* **269**, 7342 (1994)] after cleavage of the first two residues or derived from pre-PHGPx [T. R. Pushpa-Rekha, L. M. Burdsal, G. M. Chisolm, D. M. Driscoll, *ibid.* **270**, 26993 (1995)] after processing of the mitochondrial leader peptide [M. Arai *et al.*, *Biochem. Biophys. Res. Commun.* **227**, 433 (1996)]. Tryptic fragments extending toward the COOH-terminus up to position 164 were also observed with the faster migrating specimen. Charge heterogeneity may arise from phosphorylation [R. Schuckelt *et al.*, *Free Radical Res. Commun.* **14**, 343 (1991)], deaminations of Gln and Asn residues, COOH-terminal degradation, and oxidation or elimination of selenium.
16. A. Roveri, M. Maiorino, F. Ursini, *Methods Enzymol.* **233**, 202 (1994).
17. Solubilization and reduction were carried out in 0.1 M tris-HCl, 6 M guanidine-HCl, pepstatin A (0.5 μg/ml), leupeptin (0.7 μg/ml), and 0.1 M 2-mercaptoethanol at pH 7.5 and 4°C for 10 min. After centrifugation (150,000*g* for 30 min), low molecular weight compounds were removed by a NAP 5 cartridge equilibrated with 0.01 M tris-HCl, 0.15 M NaCl, 1 mM EDTA, and 1% Triton X-100 at pH 7.5. PHGPx activity

was measured at 37°C with phosphatidylcholine hydroperoxide at 3 mM GSH according to (16). Control samples were treated identically but with 5 mM 2-mercaptoethanol.

18. Other examples of "gene sharing" or "moonlighting proteins," respectively, are reviewed by J. Piatigorsky, *Prog. Ret. Eye Res.* **17**, 145 (1998); C. J. Jefferey, *Trends Biol. Sci.* **24**, 8 (1999).

19. M. Maiorino *et al.*, *Biol. Chem. Hoppe Seyler* **376**, 651 (1995); F. Ursini *et al.*, *Methods Enzymol.* **252**, 38 (1995).

20. F. Bauché, M.-H. Fouchard, B. Jégou, *FEBS Lett.* **349**, 392 (1994); R. Shalgi, J. Seligman, N. S. Kosower, *Biol. Reprod.* **40**, 1037 (1989); J. Seligman, N. S. Kosower, R. Shalgi, ibid. **46**, 301 (1992); H. M. Fisher and R. J. Aitken, *J. Exp. Zool.* **277**, 390 (1997).

21. F. Weitzel and A. Wendel, *J. Biol. Chem.* **268**, 6288 (1993); R. Brigelius-Flohé, B. Friedrichs, S. Maurer, M. Schultz, R. Streicher, *Biochem. J.* **328**, 199 (1997); P. A. Sandstrom, J. Murray, T. M. Folks, A. M. Diamond, *Free Radical Biol. Med.* **24**, 1485 (1998).

22. In other gels, mitochondrial glutathione S-transferase

23. subunit Yb-2 (accession number 121719) and endothelin converting enzyme (NCBI accession number 1706564) could be identified by MALDI-TOF or peptide sequencing.

24. Supported by the German Ministry of Education, Science and Technology, the Italian Ministry of University and Scientific Research, National Research Council, Italy, and the BIOMED 2 program of the European Community.

2 April 1999; accepted 29 July 1999

Eutrophication, Fisheries, and Consumer-Resource Dynamics in Marine Pelagic Ecosystems

Fiorenza Micheli*

Anthropogenic nutrient enrichment and fishing influence marine ecosystems worldwide by altering resource availability and food-web structure. Meta-analyses of 47 marine mesocosm experiments manipulating nutrients and consumers, and of time series data of nutrients, plankton, and fishes from 20 natural marine systems, revealed that nutrients generally enhance phytoplankton biomass and carnivores depress herbivore biomass. However, resource and consumer effects attenuate through marine pelagic food webs, resulting in a weak coupling between phytoplankton and herbivores. Despite substantial physical and biological variability in marine pelagic ecosystems, alterations of resource availability and consumers result in general patterns of community change.

Increased nutrient loadings and fisheries exploitation are major human perturbations to marine ecosystems worldwide (1). Alteration of resource availability represents a "bottom-up" perturbation of marine ecosystems, whereas removal of consumer biomass through fishing represents a "top-down" disturbance. An understanding of how bottom-up and top-down processes influence the dynamics of marine communities is necessary for effective management of marine ecosystems in the face of environmental variability and multiple human impacts. However, it is difficult to determine the effects of resource availability and food-web interactions in open (pelagic), highly variable marine systems; most propositions are based on anecdotal evidence from catastrophic events such as El Niño years (2), fishery collapses (3), and the introduction of exotic species (4). To determine how marine pelagic ecosystems respond to variation in the quantity of resources and consumers, I conducted meta-analyses of data from a variety of experimental and natural systems and examined whether changes in the abundance of consumers (pelagic zooplanktivorous fish) cascade down marine food webs to affect

lower trophic levels, and whether changes in nutrient availability and primary productivity cascade up marine food webs to affect higher trophic levels.

To address these questions, I assembled data from experimental manipulations conducted in marine mesocosms and from long-term monitoring of open marine ecosystems. Experiments conducted in mesocosms eliminate open-system dynamics but represent controlled alterations of nutrient availability and food-web structure. In contrast, long-term monitoring of open marine systems documents patterns at realistic spatial and temporal scales. The first data set comprised phytoplankton and mesozooplankton (mostly herbivorous copepod crustaceans larger than 150 to 300 μm) data from marine mesocosm experiments where nutrient availability was manipulated by adding N compounds, or where food-web structure was manipulated by adding or removing zooplanktivorous fish or invertebrates (5). The second data set consisted of time series (7 to 45 years) of N availability (measured as the annual loading or as the average N concentration during winter months), primary productivity, and the biomass of phytoplankton, mesozooplankton, and pelagic zooplanktivorous fish for 20 open marine ecosystems (6).

For the mesocosm experiments, I quantified responses of phytoplankton and mesozooplankton to nutrient and food-web manipula-

tions by using the natural logarithm of the ratio between the mean value of the variable in mesocosms with carnivores (zooplanktivorous fish or invertebrates) or nutrients (inorganic N compounds) added and in unmanipulated, control mesocosms (7). Zooplanktivores caused significant decreases in mesozooplankton biomass, both in mesocosms with no N added (Fig. 1A) and in mesocosms enriched with N (Fig. 1B). Zooplanktivores caused an increase in phytoplankton biomass, but this trend was statistically significant only in systems that were also enriched with N (Fig. 1, A and B). Nitrogen addition caused similar and significant increases in phytoplankton biomass in mesocosms containing two (phytoplankton and zooplankton; Fig. 1C) or three trophic levels (phytoplankton, zooplankton, and zooplanktivores; Fig. 1D). Under either food-web configuration, nutrient addition did not affect mesozooplankton biomass (Fig. 1, C and D). The effects of the manipulations were not significantly correlated with either experiment duration or mesocosm size in zooplanktivore-manipulation experiments (8), and the effects were only weakly correlated with duration but not with size in nutrient-manipulation experiments (9). Therefore, these results are unlikely to be biased by the short duration or small mesocosm sizes used in most experiments.

For the 20 open marine ecosystems, I examined the cross-correlation between time series of nutrients, productivity, and biomass of different trophic levels using Spearman rank correlation (10). Theoretical models exploring the relations among resource availability, food-web structure, and biomass of different trophic levels predict patterns of biomass accrual along productivity gradients at equilibrium, that is, after transient effects have disappeared (11, 12). Because seasonal events such as upwelling and sudden increases in fish density from immigration or spring reproduction are transient effects, I used yearly values of productivity and biomass to approximate equilibrium conditions. Year-to-year fluctuations in mesozooplankton biomass were negatively correlated with zooplanktivorous fish ($r = -0.22$; 95% confidence limits $= -0.31$ and -0.12; $N = 19$), indicating that fish predation may control mesozooplankton biomass. In contrast, the correlation between mesozooplankton and

National Center for Ecological Analysis and Synthesis, Santa Barbara, CA 93101, USA.

*Present address: Dipartimento di Scienze dell'Uomo e dell'Ambiente, Universita' di Pisa, 56126 Pisa, Italy. E-mail: f.micheli@trident.nettuno.it